HYDROLOGICAL PROCESSES
Hydrol. Process. **25**, 141–151 (2011)
Published online 1 September 2010 in Wiley Online Library
(wileyonlinelibrary.com) DOI: 10.1002/hyp.7833

Trench infiltration for managed aquifer recharge to permeable bedrock†

Victor M. Heilweil[1]* and Dennis E. Watt[2]

[1] *U.S. Geological Survey, 2329 Orton Circle, Salt Lake City, UT 84119, USA*
[2] *U.S. Bureau of Reclamation, Lower Colorado Regional Office, PO Box 61470, Boulder City, NV 89006-1470, USA*

Abstract:

Managed aquifer recharge to permeable bedrock is increasingly being utilized to enhance resources and maintain sustainable groundwater development practices. One such target is the Navajo Sandstone, an extensive regional aquifer located throughout the Colorado Plateau of the western United States. Spreading-basin and bank-filtration projects along the sandstone outcrop's western edge in southwestern Utah have recently been implemented to meet growth-related water demands. This paper reports on a new cost-effective surface-infiltration technique utilizing trenches for enhancing managed aquifer recharge to permeable bedrock. A 48-day infiltration trench experiment on outcropping Navajo Sandstone was conducted to evaluate this alternative surface-spreading artificial recharge method. Final infiltration rates through the bottom of the trench were about 0·5 m/day. These infiltration rates were an order of magnitude higher than rates from a previous surface-spreading experiment at the same site. The higher rates were likely caused by a combination of factors including the removal of lower permeability soil and surficial caliche deposits, access to open vertical sandstone fractures, a reduction in physical clogging associated with silt and biofilm layers, minimizing viscosity effects by maintaining isothermal conditions, minimizing chemical clogging caused by carbonate mineral precipitation associated with algal photosynthesis, and diminished gas clogging associated with trapped air and biogenic gases. This pilot study illustrates the viability of trench infiltration for enhancing surface spreading of managed aquifer recharge to permeable bedrock. Published in 2010 by John Wiley & Sons, Ltd.

KEY WORDS trench infiltration; managed aquifer recharge; fractured sandstone; trapped gas; seasonal viscosity variation

Received 22 November 2009; Accepted 23 June 2010

INTRODUCTION

Applying managed aquifer recharge to permeable bedrock is becoming an increasingly common practice (Reese, 2001; Dillon, 2005; Mhamdi and Heilweil, 2007; Brand, 2008). While aquifer storage and recovery (ASR) using injection wells is presently the primary method utilized for bedrock aquifers (Pyne, 2005), surface spreading can be more efficient and cost effective (Chadha, 2000). Spreading-basin and bank-filtration recharge, however, is often inhibited by clogging. Both siltation (Rice, 1974; Bouwer, 1996) and biofilm development (Katznelson, 1989; Baveye *et al*., 1998; Rinck-Pfeiffer *et al*., 2000) can reduce recharge at spreading basins that utilize source water having either a high-suspended sediment load or warm nutrient-rich water. Reduced infiltration rates of two to three orders of magnitude, caused by physical clogging associated with siltation, have been reported (Dilyunas, 1976; Schuh, 1988). Bubbles from trapped air associated with the wetting front or incorporated in otherwise saturated porous media have been shown to cause up to a tenfold decrease in permeability (Christiansen, 1944; Constantz *et al*., 1988; Faybishenko, 1995; Heilweil *et al*., 2004). Biogenic gases produced during bacterial/microbial respiration, decay, and denitrification (Oberdorfer and Peterson, 1985; Beckwith and Baird, 2001; Waddington *et al*., 2009) can clog pore spaces and have been linked with seasonal decreases in infiltration during warmer summer months (Heilweil *et al*., 2009b). The increased dynamic viscosity associated with cooler water temperature has been shown to reduce effective hydraulic conductivity (Cho *et al*., 1999) and reduce spreading-basin infiltration during cooler winter months at higher latitudes (Schuh, 1990). Carbonate precipitation is often associated with increased pH of reservoir water caused by algal consumption of bicarbonate during photosynthesis. Such calcite precipitation is often observed with spreading basins (Escalante *et al*., 2009) and has been shown to cause cementation and clogging of sediments beneath surface-spreading basins and permeability reduction (Bouwer and Rice, 1984, 1989). An artificial recharge infiltration study by Schuh (1990) reported clogging associated with carbonate precipitation and cementation in soils beneath a surface-spreading basin with an associated increase in pH to about 9. Additionally, evaporative losses from surface reservoirs can be substantial, particularly in the warm and dry climate of the southwestern United States (Morton, 1983; Paulson, 1983; Barnett and Pierce, 2008). Evaporative losses at Sand Hollow Reservoir in southwestern Utah approach 0·01 m/day during the warmer

* Correspondence to: Victor M. Heilweil, U.S. Geological Survey, 2329 Orton Circle, Salt Lake City, UT 84119, USA. E-mail: heilweil@usgs.gov
† This article is a US Government work and is in the public domain in the USA.

summer months and 1·7 m annually (Heilweil *et al.*, 2009a).

Infiltration trenches (including ditches, shafts, and pits) for surface-water recharge hold promise for reducing both clogging effects and evaporative losses. While trench infiltration has been extensively documented for recharge to unconsolidated soils and aquifers (Smith, 1967; Hantke and Schlegel, 1995; Gale and Dillon, 2005; Dagès *et al.*, 2008; National Research Council, 2008), its use for enhancing recharge to bedrock has not previously been reported. The purpose of this study was to evaluate the performance of infiltration trenches as an alternative surface-based approach to spreading-basin techniques for managed aquifer recharge to permeable bedrock.

HYDROGEOLOGICAL SETTING AND PREVIOUS STUDIES

The Navajo is a well-sorted eolian sandstone and is part of the Dakota-Glen Canyon aquifer system, having an areal extent of about 500 000 km^2 in the Colorado Plateau Physiographic Province of Arizona, Colorado, Utah, and Wyoming in the western United States (Robson and Banta, 1995). Its thickness in southwestern Utah reaches up to 850 m, with a maximum thickness of 350 m in Sand Hollow (Hurlow, 1998). Its near-vertical fractures have an average horizontal spacing of 5 m, with apertures of up to 20 mm (RBG Engineering, written commun., 2003). These fractures are generally filled with secondary caliche (calcium carbonate) deposits associated with plant-root transpiration to depths of about 2·5 m, but are generally open at greater depths (Figure 2a; Heilweil and Solomon, 2004). The sandstone is either exposed or covered with a thin (<3 m) layer of sandy loam or silty sand and the top 0·5 m is weathered and poorly cemented (Heilweil *et al.*, 2007).

Total porosity and saturated vertical hydraulic conductivity values from laboratory analyses were previously reported for soils, caliche, and sandstone at the infiltration trench experiment site in Sand Hollow basin (Heilweil *et al.*, 2004). The porosity of 14 unconsolidated soil samples ranged from 0·29 to 0·45 with an arithmetic mean of 0·39 (Table I). Saturated vertical hydraulic conductivity values for these soils ranged from 0·004 to 0·06 m/day with a geometric mean of 0·02 m/day. The porosity of three caliche samples ranged from 0·10 to 0·32, with an arithmetic mean of 0·21. Saturated hydraulic conductivity of these caliche samples ranged from 0·0002 to 0·008 m/day, with a geometric mean of 0·006 m/day. The porosity of four shallow weathered sandstone core samples collected from a depth of ~1 m ranged from 0·20 to 0·26, with an arithmetic mean of 0·22. Saturated hydraulic conductivity of these weathered sandstone samples ranged from 0·10 to 0·23 m/day with a geometric mean of 0·17 m/day. The porosity of 13 deeper non-weathered sandstone core samples collected from depths of 2 to 19 m ranged from 0·20 to 0·27, with an arithmetic mean of 0·24. Saturated hydraulic conductivity of these non-weathered sandstone samples ranged from 0·01 to 0·42 m/day, with a geometric mean of 0·10 m/day. These previous data indicate that unconsolidated soils and caliche have lower saturated hydraulic conductivity than the underlying weathered and nonweathered sandstone. Results from these sandstone core samples represent only matrix permeability. A series of Navajo Sandstone multiple-well aquifer tests in and around Sand Hollow yielded a range of bulk (matrix plus fracture) horizontal hydraulic conductivity values of 0·1 to 10 m/day. While the lower end of this range is the same as the mean laboratory vertical hydraulic conductivity, the higher values are attributed to fractures within the sandstone. This fracturing resulted in a horizontal anisotropy ranging from 3 : 1 at Gunlock, Utah, about 40 km west of Sand Hollow (Heilweil *et al.*, 2000, Appendix A), up to 32 : 1 at Anderson Junction about 20 km north of Sand Hollow (Heilweil and Hsieh, 2006).

Horizontal-to-vertical anisotropy of the Navajo Sandstone aquifer is assumed to be negligible based on previous laboratory measurements and regional numerical groundwater flow modelling. Reported laboratory horizontal and vertical saturated hydraulic conductivity values of three Navajo Sandstone samples from Zion National Park, about 30 km east of the study area, ranged from 0·54 to 1·0 m/day and 0·01 to 1·5 m/day, respectively (Uygur, 1980; Freethey, 1988). Reported laboratory horizontal and vertical saturated hydraulic conductivity values of 11 samples from Kanab, about 60 km east of the study area, ranged from 0·04 to 1·8 m/day and 0·003 to 1·5 m/day, respectively (Freethey, 1988). Regional groundwater flow models of both an area including Sand Hollow (Heilweil *et al.*, 2000) and in the Zion National Park area (Heilweil and Freethey, 1992) did not require the use of horizontal-to-vertical anisotropy factors for model calibration.

Previously reported Navajo Sandstone storage coefficients determined from multiple-well aquifer testing ranged from 0·001 to 0·002 (Heilweil *et al.*, 2000).

Table I. Laboratory-determined porosity (φ) and saturated vertical hydraulic conductivity (K_v) of material at the infiltration trench experiment site, Sand Hollow, Utah

Material	Number of samples	Minimum φ	Maximum φ	Arithmetic mean φ	Minimum K_v, in m/day	Maximum K_v, in m/day	Geometric mean K_v, in m/day
Unconsolidated soils	14	0·29	0·45	0·39	0·004	0·06	0·02
Caliche deposits	3	0·10	0·32	0·21	0·0002	0·008	0·0006
Weathered sandstone	4	0·20	0·26	0·22	0·10	0·23	0·17
Non-weathered sandstone	13	0·20	0·27	0·24	0·01	0·42	0·10

Because these values were determined from short-duration aquifer tests, they likely represent confined conditions without substantial dewatering of the sandstone pores. It is assumed that unconfined storage values of the Navajo Sandstone determined from longer-term aquifer testing would approach effective porosity. A mean effective porosity value of 0·17 was reported by Cordova (1978), based on laboratory measurements of Navajo Sandstone samples collected from 12 outcrop sites in southwestern Utah near Sand Hollow.

While managed aquifer recharge to the Navajo Sandstone of southwestern Utah was first introduced in 2002 as surface-basin infiltration at Sand Hollow (Figure 1), unmanaged aquifer recharge, as defined by Dillon (2009), had already been occurring for decades through induced bank filtration. Induced bank filtration is the process by which seepage from a surface-water body (such as a river or lake) to an aquifer is induced by nearby extraction wells (Hiscock and Grischek, 2002; Massmann and Sültenfuß, 2008). At Gunlock, Utah, groundwater recharge to the Navajo Sandstone from the adjacent Gunlock Reservoir and Santa Clara River has been induced by pumping of public supply production wells since the 1970s, as confirmed by environmental tracers (chlorofluorocarbons) and aquifer testing (Heilweil *et al.*, 2000).

Sand Hollow Reservoir is conjunctively operated for both surface-water storage and as a spreading basin for managed aquifer recharge to the underlying Navajo Sandstone. From 2002 through 2007, it is estimated that more than 80 million cubic meters (80 Mm^3) of seepage through the bottom of the reservoir has entered the aquifer

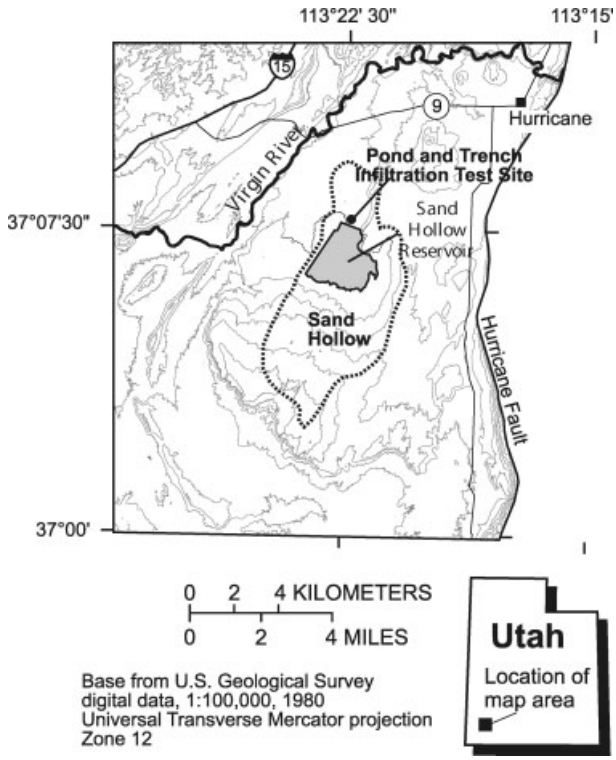

Figure 1. Location of the pond and trench infiltration test site in Sand Hollow, Utah

(Heilweil *et al.*, 2005, 2009a). Estimated evaporation from Sand Hollow Reservoir for this same period was 30 million cubic meters (30 Mm^3), and has been increasing in recent years and approaching managed aquifer recharge quantities because above-average precipitation and inflow during 2004–2005 resulted in the reservoir remaining nearly full and near its surface-area maximum (Heilweil *et al.*, 2009a).

Prior to the construction of Sand Hollow Reservoir, a 260-day infiltration pond surface-spreading experiment was conducted just north of the reservoir site (Heilweil *et al.*, 2004). The circular pond had a radius of 30 m and was situated on about 1 m of undisturbed soils overlying sandstone. A 0·1 to 0·5 m layer of caliche was observed at the soil/sandstone contact and in the underlying weathered sandstone; caliche was also present in the shallow parts of sandstone fractures (Figures 2a,2b). Prior to the experiment, the regional water table in the Navajo Sandstone aquifer was at a depth of about 22 m below land surface. During the infiltration pond experiment, the water table rose by almost 2 m to a depth of about 20 m, but never connected with the perched water directly beneath the pond. Excluding the initial 7-day wetting-up period, the average infiltration rate during the infiltration pond experiment was about 0·05 m/day.

This paper discusses a follow-up trench experiment conducted at the same infiltration pond site in Sand Hollow to test the hypothesis that infiltration rates could be increased by (1) bypassing lower permeability soils and caliche deposits and accessing open near-vertical fractures, (2) maintaining isothermal water temperatures, (3) minimizing siltation and biofilm development, (4) minimizing clogging associated with mineral precipitation, and (5) reducing trapped air effects by reducing biogenic gas production and increasing lateral outward gas dissipation.

INFILTRATION TRENCH EXPERIMENT METHODOLOGY

After completion of the infiltration pond experiment, about 1·5 m of soil, caliche deposits and weathered sandstone were scraped off the site in preparation for the infiltration trench experiment. A 1-m wide by 3-m deep 'T'-shaped trench, having a total length of about 90 m and surface area of about 90 m^2, was then cut into the underlying Navajo Sandstone (Figures 2c and 3). The 3-m depth of the trench was considered particularly important because it allowed direct access to open fractures (without caliche infill). The trench was partially backfilled with 2 m of gravel. A horizontal perforated 20-cm diameter polyvinyl chloride (PVC) pipe was laid upon this gravel (Figure 3) and connected to a pipeline from the Wayne Wilson well (screened in the Navajo Sandstone about 1000 m northeast of the test site), which provided water that was geochemically similar to the native groundwater beneath the trench (Heilweil *et al.*, 2005). The perforated pipe was then

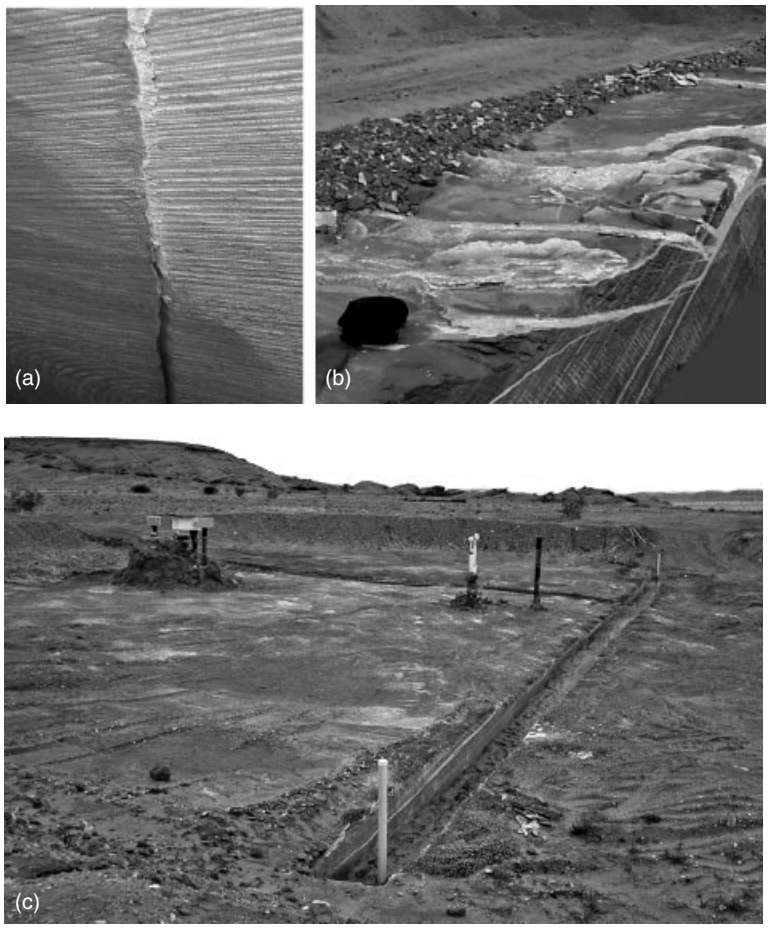

Figure 2. Photographs showing (a) caliche fill in vertical fracture to 2·5 m depth, (b) caliche deposits at soil/sandstone contact, and (c) infiltration trench experiment site, Sand Hollow, Utah

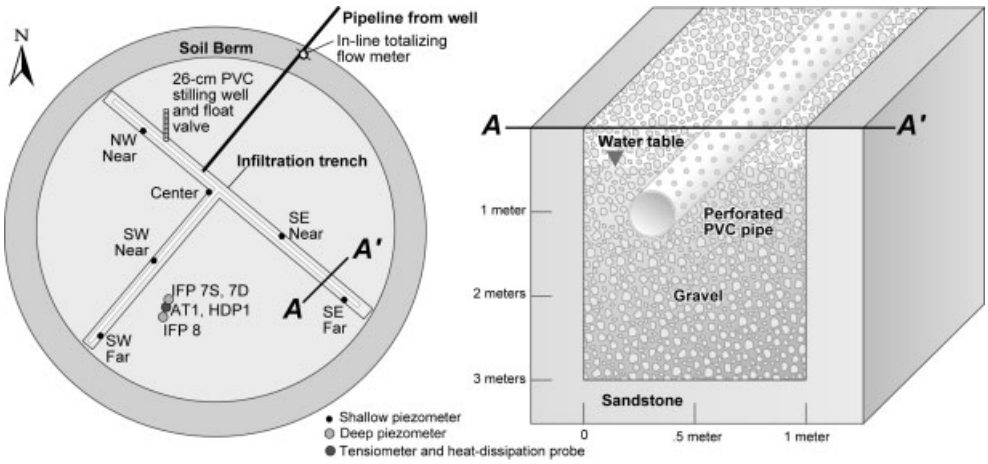

Figure 3. Map view and cross-section of infiltration trench experiment site at Sand Hollow, Utah

covered by an additional 1 m of gravel. An in-line totalizing meter measured inflow to the trench. Water levels were regulated by a 26-cm diameter stilling well and float system installed in the trench that was wired to trigger pumping from the nearby well when the water level dropped to 0·4 m beneath the top of the trench; a shut-off float stopped pumping once the water level reached a height of 0·25 m beneath the top of the trench. The water level in the trench, therefore, fluctuated by about 0·15 m between filling cycles. Evaporation was minimized by maintaining water levels beneath the top of the gravel fill in the trench to avoid atmospheric exposure.

Six shallow piezometers installed within the infiltration trench and three deeper nearby piezometers in the underlying sandstone were used to measure water levels and vertical hydraulic gradients in both the trench and the underlying sandstone during the experiment (Figure 3). The center piezometer was also used for measuring

temperature and pH of water in the trench. The shallow piezometers were constructed from 2·2-cm diameter PVC pipe, each with a total depth of 3·5-m and a 15-cm long-screened interval at the base of the trench. These were used to ensure that the trench was saturated throughout the experiment. The deeper infiltration pond (IFP) piezometers (IFP 8, IFP 7S, and IFP 7D) were all located about 5 m from the trench and screened at depths of 2·4–3·9 m, 16·5–18·0 m, and 18·9–20·4 m, respectively, beneath the top of the trench, which corresponded to the soil/sandstone contact. Before beginning the infiltration trench experiment, depth to water was about 5 m below the top of the trench. The regional water table had risen 15 m since the prior pond experiment because of managed aquifer recharge from the nearby reservoir.

Pairs of tensiometers and heat dissipation probes were installed at various depths in the sandstone about 5 m from the trench to measure water potential of the sandstone matrix (Figure 3). Only the shallowest advanced tensiometer (AT1) and heat dissipation probe (HDP1) pair were located above the regional water table at the start of the infiltration trench experiment (at depths of 4·1 and 4·4 m beneath the top of the sandstone, respectively). The advanced tensiometer used for this experiment measures soil-water potential below land surface and consists of a permanently installed outer assembly with a porous cup, water reservoir, and guide pipe along with a removable electronic pressure transducer assembly that connects and seals to the outer assembly (Hubbell and Sisson, 1998). The transducer can measure both tension (negative water potential) and hydraulic head (positive water potential). The HDP1 consists of a porous block, a pulse-heated point, and a thermistor. Temperature is measured both before and after a small heat pulse is applied; this temperature difference (heat flow) is proportional to the amount of water in the porous media (Bristow *et al.*, 1993). Unlike the advanced tensiometer, the HDP1 only measures negative water potential, not hydraulic head.

RESULTS

Volumetric flux rates

The infiltration trench experiment was conducted for 48 days, during which time approximately 2000 m^3 of recharge occurred (Table II). Volumetric flux rates were calculated by dividing the difference in volumetric flow recorded by the inflow meter by the time segment, in days. The resulting volumetric flux rates were divided into three periods (Figure 4). Phase 1 (0–5 days) consisted of a rapid decrease from about 150 to 45 m^3/day, corresponding to the saturation of the sandstone in the immediate vicinity of the trench. During Phase 2 (5–40 days), flux rates gradually decreased from about 43 to 33 m^3/day as the wetting front progressed towards the water table. During Phase 3 (40–48 days), flux rates remained steady at about 33 m^3/day after a saturated hydraulic connection was established between the trench and the regional water table.

Water-level, hydraulic-gradient, and water-potential data

During the experiment, the water level in the aquifer beneath the trench rose by about 2·5 m. Water levels in, and vertical hydraulic gradients between the three deep piezometers show different responses to infiltration (Figures 5 and 6). Similar to the shallow piezometers in the trench, IFP 8 (bottom of screen at 3·9 m below the top of the trench) was initially dry before the start of the trench experiment. This was consistent with initial water levels at piezometers IFP 7S and IFP 7D of about 4·9 m below the top of the trench. Piezometer IFP 8 became saturated (water level about 3·8 m below the top of the trench) about 1 day after the experiment began and water levels continued to rise until the end of the experiment. In contrast, water levels in the IFP 7S and IFP 7D piezometers remained at about 4·9 m below the top of the trench until 18 days, indicating the existence of a 1-m thick vadose zone during the first part of the experiment.

The vadose-zone water potential, measured by the advanced tensiometer and heat dissipation probes, also shows the steady downward progression of the wetting front (Figure 7). The AT1 reached saturation at 27 days. Prior to 27 days, this tensiometer recorded negative pressures as low as −80 cm of water, indicating unsaturated conditions. Between 27 days and 40 days, the tensiometer recorded positive pressures up to +70 cm of water, indicating saturated conditions. The adjacent but deeper HDP1 reached saturation at about 35 days, as indicated by matric potential values approaching 0 bars. Prior to 35 days, the heat dissipation probe recorded matric potentials as low as $-0 \cdot 06$ bars.

Infiltration trench rates

Infiltration rates (seepage flux rates; (L/T)), determined by dividing the metered volumetric inflow rate (L^3/T) to the trench by the 90 m^2 cross-sectional area of the bottom of the trench, rapidly declined from 1·8 to 0·76 m/day during the initial 4-day wetting-up period of the experiment (Table II, Figure 4). The mean infiltration rate during Phase 2 (days 5–40) of the experiment was $0{\cdot}51 \pm 0{\cdot}015$ m/day (2σ). This rate decreased to a mean of 0·39 m/day $\pm 0{\cdot}009$ m/day (2σ) during Phase 3 (days 40–48), when the water in and near the trench became hydraulically connected to the regional aquifer.

The increase in water levels at piezometers IFP 7S and IFP 7D at 18 days indicates that some recharge from the trench moved through the vadose zone and reached the regional water table during Phase 2 of the experiment (Figure 5). This is also indicated by an increase in the downward vertical hydraulic gradient between IFP 7S and IFP 7D at 18 days (Figure 6). Such recharge likely

Table II. Volumetric inflow rate, infiltration rate, water temperature, and pH during the infiltration trench experiment, Sand Hollow, Utah

Elapsed time (days)	Totalizing meter (m^3)	Segment volume (m^3)	Volumetric inflow rate (m^3/day)	Infiltration rate (m/day)	Center piezometer water temperature (°C)	Center piezometer pH
0·0	17	0	0	0	—	—
0·3	65	48	149	1·77	—	—
0·8	113	48	94	1·12	—	—
1·3	152	39	79	0·93	16·3	7·6
1·9	188	36	67	0·79	—	—
2·1	203	15	66	0·78	—	—
2·8	253	50	66	0·78	—	—
3·9	318	65	64	0·76	—	—
4·9	363	46	43	0·51	—	—
6·2	416	52	43	0·51	—	—
7·1	455	39	43	0·51	16·6	7·8
8·1	499	44	43	0·51	—	—
8·9	533	34	43	0·51	—	—
9·8	573	40	42	0·50	—	—
10·9	618	45	43	0·51	—	—
12·0	666	47	42	0·50	—	—
12·9	705	40	43	0·51	—	—
14·1	755	49	42	0·50	16·2	7·9
14·9	790	36	43	0·51	—	—
15·9	833	42	42	0·50	—	—
16·9	872	39	43	0·51	—	—
18·0	922	50	43	0·51	—	—
19·0	965	43	43	0·51	—	—
19·9	1004	39	43	0·51	—	—
20·9	1046	42	43	0·51	16·1	7·7
21·9	1086	40	43	0·51	—	—
22·0	1091	5	44	0·52	—	—
23·9	1174	83	42	0·50	—	—
25·9	1259	85	44	0·52	—	—
28·0	1351	91	44	0·52	15·9	8·1
29·9	1439	88	45	0·53	—	—
30·9	1479	40	43	0·50	—	—
33·1	1567	88	40	0·47	—	—
35·9	1683	116	40	0·48	15·7	7·8
37·1	1730	46	41	0·49	—	—
38·0	1767	37	39	0·46	—	—
40·0	1832	65	33	0·39	—	—
42·0	1899	67	33	0·40	15·6	8·2
43·0	1930	31	33	0·39	—	—
44·0	1967	37	35	0·41	—	—
46·9	2064	97	33	0·40	—	—
48·0	2097	33	32	0·38	15·8	7·7

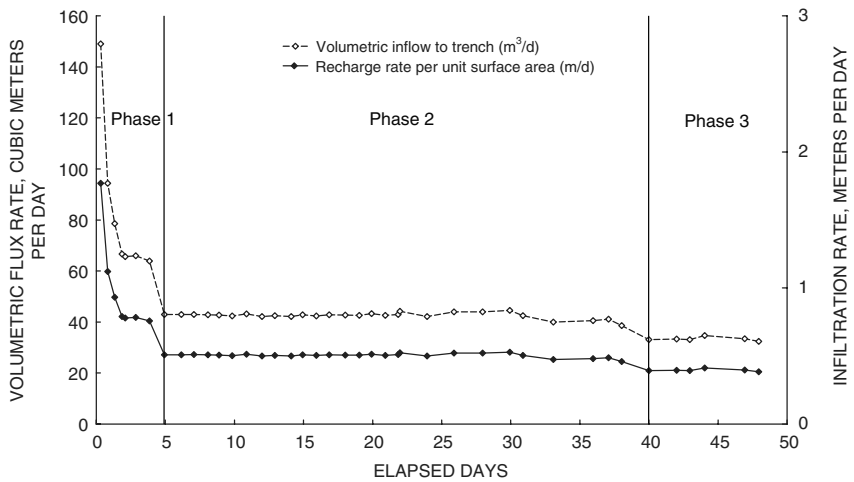

Figure 4. Volumetric inflow and infiltration rates during the infiltration trench experiment at Sand Hollow, Utah

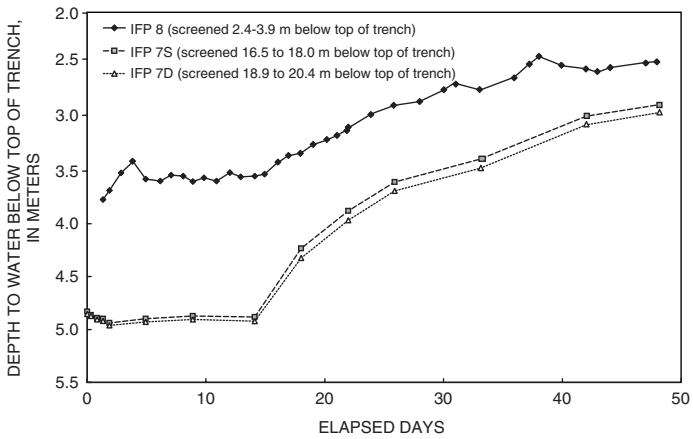

Figure 5. Water levels in deep piezometers during the infiltration trench experiment at Sand Hollow, Utah

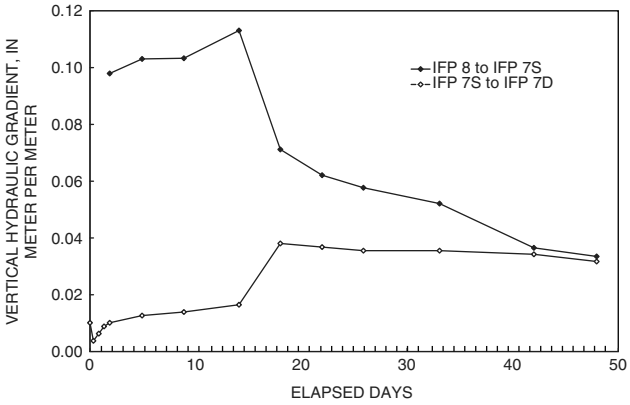

Figure 6. Vertical hydraulic gradients calculated from water levels in the deep piezometers during the infiltration trench experiment at Sand Hollow, Utah

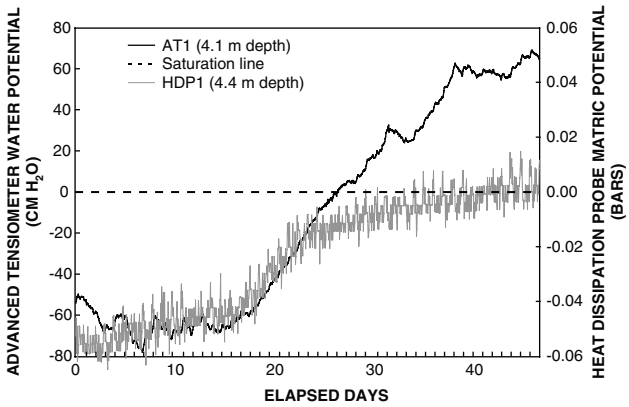

Figure 7. AT1 and HDP1 measurements during the infiltration trench experiment at Sand Hollow, Utah

reached the regional water table as preferential flow along fractures, rather than as a wetting front within the sandstone matrix. This is consistent with evidence of preferential flow during the prior infiltration pond experiment, in which a bromide tracer added to the initial pond water was detected in monitoring wells in the regional aquifer weeks before the sandstone matrix reached steady-state saturation. A thin ($\leq$1 m) vadose zone between the trench and the regional water table persisted until about 42 days, as shown by the larger vertical hydraulic gradient between piezometers IFP 8 and IFP 7S, compared to IFP 7S and IFP 7D. After 42 days, the vertical hydraulic gradients between piezometers IFP 7S, IFP 7D, and IFP 8 were all similar at about 0·03 m/meter indicating complete saturation of the sandstone matrix. While the water-level data from the deep piezometers show changes at 18 days, when recharge (presumably as preferential flow) first reached the regional water table, the volumetric inflow rate shows an abrupt decrease after 4 days (Figure 4). This earlier decrease perhaps indicates that sandstone saturation and hydraulic connection to the regional water table directly beneath the trench occurred earlier than at the 5-m horizontal distance from the trench where the deeper piezometers were located.

Water-quality measurements

Water temperature and pH were measured approximately weekly in the center piezometer throughout the infiltration trench experiment (Figure 3, Table II). Water temperature varied between 15·6 and 16·6 °C. These temperatures were slightly cooler than both the measured temperature (21 °C) of the Wayne Wilson supply well and an average temperature of $18{\cdot}3 \pm 1{\cdot}4$ °C (2σ) of other measurements ($n = 42$) from wells within Sand Hollow (Heilweil *et al.*, 2009a, Table I). Some cooling likely occurred when the groundwater was transported through the above-ground pipeline to the infiltration trench site as a result of lower air temperatures during late autumn when the test was conducted. The pH of water in the trench varied between 7·6 and 8·2 throughout the experiment, similar to previously measured pH values of 7·6–8·0 of groundwater from the supply well (Heilweil *et al.*, 2005) and an average pH value of $7{\cdot}8 \pm 1{\cdot}4$ (2σ) of other groundwater pH measurements ($n = 50$) from wells within Sand Hollow (Heilweil *et al.*, 2009a, Table I). Finally, algal growth was not observed in water samples collected from the center piezometer during the infiltration trench experiment.

DISCUSSION

Infiltration rates during the trench experiment at Sand Hollow were about an order of magnitude larger than rates during the previous infiltration pond experiment (0·05 m/day; Heilweil *et al.*, 2004). These higher rates are likely due to the combined effects of (1) the geometry of the seepage face, (2) removing lower-permeability soil/caliche deposits and accessing open sandstone fractures, (3) maintaining warmer isothermal conditions resulting in a lower average dynamic viscosity and higher average hydraulic conductivity, (4) minimizing physical clogging caused by silt and biofilm layers, (5) minimizing clogging associated with carbonate mineral precipitation, and (6) reducing the clogging effects of trapped gas bubbles. In addition, minimizing evaporative loss by avoiding atmospheric exposure also resulted in more efficient water use compared with other surface-spreading methods in Sand Hollow.

The linear geometry of the trenches and the increased surface area of the seepage face between the trench and the underlying water table may partly explain the higher infiltration rates found during the trench experiment. The infiltration trench's linear shape yields a plan-view perimeter/surface-area ratio of about 2·0 (180-m total length of trench walls divided by 90 m^2 plan-view area) compared to the infiltration pond's circular shape (30-m radius) and plan-view circumference/surface-area ratio of about 0·07. Because of this larger perimeter/surface-area ratio, for an equal depth to the water table, the 1-m wide linear infiltration trench had about 30 times more sandstone contact area than the infiltration pond. The actual footprint of the linear recharge mound on the regional water table beneath an infiltration trench will be a function of the transmissivity and storage properties of the sandstone and the depth to the water table beneath land surface. Optimizing the lateral spacing of a gallery of parallel infiltration trenches to maximize recharge could be evaluated with multiphase (unsaturated/saturated) groundwater flow modelling.

Removal of the lower-permeability soils and caliche deposits (present beneath the infiltration pond experiment) prior to the infiltration trench experiment is likely an important factor in the higher trench infiltration rates. The mean vertical saturated hydraulic conductivity from laboratory measurements of these soil and caliche deposits was lower (0·02 and 0·0006 m/day, respectively) than the mean values for weathered and non-weathered sandstone (0·17 and 0·10 m/day, respectively). In addition, accessing open fractures near the bottom of the trench (compared with the caliche-filled shallow parts of these fractures) was also a factor contributing to the improved results of the trench experiment.

The water in the trench during the experiment (conducted from 27 October 2004 to 14 December 2004) remained at a relatively constant temperature of about $16{\cdot}1 \pm 0{\cdot}5\,^{\circ}C$, warmer than the mean water temperature (11·1 °C) of the infiltration pond experiment during the same time period (late autumn) in the year 2000. Both experiments used the same groundwater source and pipeline. Meteorological records from a weather station in Sand Hollow indicate that mean air temperature during these two time periods was very similar (6·8 °C in 2000; 7·7 °C in 2004). The water in the trench was warmer than the pond because it was not exposed to the cooler atmosphere while in the trench. The dynamic viscosity of water decreases from 1·27 centipoise at 11 °C to 1·11 centipoise at 16 °C. This decrease results in a 14% increase in hydraulic conductivity. If the trench experiment had been conducted during the early winter (from December to January 2000, the average pond temperature was 6·7 °C with a dynamic viscosity of 1·44 centipoise), the decrease in dynamic viscosity using trench infiltration with 16 °C isothermal water would cause a hypothetical 30% increase in hydraulic conductivity and infiltration rates.

Compared to surface spreading during both the infiltration pond experiment and at Sand Hollow Reservoir, physical clogging associated with siltation and organic biofilm formation was minimized during the infiltration trench experiment. Three potential sources of silt to Sand Hollow Reservoir include suspended sediments in the inflowing surface water, eolian dust transport, and reworking of pre-existing sediments by wave action along the bottom of the reservoir (Heilweil *et al.*, 2009b). During both the pond and trench experiments, the rate of siltation was likely less than in Sand Hollow Reservoir because of the lower suspended-sediment load of the groundwater from the nearby well, compared to the surface-water inflow to the reservoir from the Virgin River. Siltation from eolian dust transport and reworking of sediments by wave action were factors that likely reduced infiltration during the infiltration pond experiment (open system) but not during the infiltration trench experiment (closed system). Furthermore, any silt that entered the trench likely moved downward through the gravel backfill and settled along the trench bottom. With longer-term use, the floor of the trench may eventually become sealed by a silt layer, but the vertical sandstone walls and open fractures in the lower part of the trench would remain silt-free. Because water was not exposed to the sun, no algal growth was observed in the trench and it is assumed that no physical biofilm clogging occurred during the infiltration trench experiment. In contrast, pelagic and benthic algal growth were observed in the surface waters of both the infiltration pond and Sand Hollow Reservoir.

Clogging from carbonate mineral precipitation has been linked to increasing pH associated with algal photosynthesis at other artificial recharge infiltration study sites (Bouwer and Rice, 1984, 1989; Schuh,1990). Carbonate mineral precipitation along the perforated PVC pipe in the trench was not evaluated during the infiltration trench experiment. The lack of solar exposure, absence of algal growth, and near-neutral pH of water in the trench, however, suggest that such clogging did not occur during the experiment. The pH values of 7·6–8·1, measured in the center piezometer during the infiltration

trench experiment, were lower than previously reported pH values of water from Sand Hollow Reservoir (pH of 8·1–8·8; Heilweil *et al.*, 2009a) and of pore water in temporary piezometers installed in the silt layer beneath the reservoir (pH up to 8·7; Heilweil *et al.*, 2009b).

Compared to surface-spreading techniques, trench infiltration should be less affected by clogging associated with trapped air and biogenic gas bubbles. During the infiltration pond experiment at Sand Hollow, clogging by trapped air bubbles in the otherwise-saturated pore spaces was shown to substantially reduce permeability and infiltration rates. Much of this initially trapped air (comprised primarily of nitrogen) eventually dissipated laterally or dissolved and there was a twofold increase in permeability beneath the pond from day 60 (late September) to day 150 (late December) as pond temperatures cooled from about 30 to 5 °C, resulting in an increase in nitrogen solubility from 9·1 to 14·8 cm^3/kg (Heilweil *et al.*, 2004, Figure 6). Calculations indicated that it would take approximately 500 days to completely dissolve the air bubbles initially trapped beneath the pond assuming an average temperature of 20 °C and no lateral dissipation. Similar calculations for the infiltration trench experiment show that trapped gas dissolution would occur much faster. With the same assumptions used for the infiltration pond experiment (a 2-m thick layer of saturated sandstone having 10% of its porosity filled with trapped air bubbles) and an estimated non-weathered sandstone porosity of 24% (Heilweil *et al.*, 2004), the volume of air bubbles initially trapped beneath the 90 m^2 trench bottom was estimated to be 4 m^3 (4×10^6 cm^3). Based on a nitrogen solubility of 11·6 cm^3/L in 16 °C water (determined from Weiss, 1970) at 0·9 atmosphere pressure (experiment site elevation = 900 m) and assuming an increase in nitrogen solubility of 5 cm^3/L due to increased hydrostatic head at a water depth of 4 m beneath the top of the trench, it would take approximately 930 000 L of recharge to entirely dissolve the trapped air bubbles. Using the measured volumetric inflow rate of 32 000 L/day(32 m^3/day; Table II) at the end of the infiltration trench experiment, it would only take about 28 days for the trapped air bubbles beneath the trench to completely dissolve—a nearly 20-fold reduction compared to the infiltration pond experiment. The geometry of pond and trench infiltration may also influence the lateral dissipation of trapped gas. The infiltration pond's circular shape and 30-m radius yields a plan-view circumference/surface-area ratio of about 0·07 compared to the trench bottom's perimeter/surface-area ratio of about 2·0 (180-m total length of trench walls divided by 90 m^2 plan-view area). Because of this larger perimeter/surface-area ratio, air bubbles trapped beneath the trench during the initial wetting period may also more readily dissipate laterally. Another gas-clogging consideration for managed aquifer recharge via surface spreading is the production of biogenic gases from algal growth. Dissolved-gas sampling in temporary piezometers installed beneath Sand Hollow Reservoir documented the presence of trapped gas bubbles containing high concentrations of CO_2 and CH_4 derived from algal biofilm respiration and decay (Heilweil *et al.*, 2009b). While dissolved gas concentrations were not evaluated during the infiltration trench experiment, it is assumed that the lack of solar exposure and algal growth in this setting would minimize biogenic gas production and associated gas clogging.

In addition to higher sustained rates, trench infiltration will utilize water more efficiently (less evaporation) than spreading basins and cost less per unit recharge volume than ASR injection wells. While average evaporation rates during the trench experiment (November–December 2004) were only 0·0006–0·001 m/day (based on estimated evaporation rates of 0·03 and 0·02 m/month for the nearby Sand Hollow Reservoir; Heilweil *et al.*, 2009a), evaporation during the previous infiltration pond experiment reached a maximum of 0·042 m/day in August 2000, nearly as high as the mean infiltration rate of 0·055 m/day (Heilweil *et al.*, 2004). This indicates that water-use efficiency (infiltration rate divided by evaporation rate) was as low as 1·3 during the warmer months of the pond experiment. Water-use efficiency for artificial recharge beneath Sand Hollow Reservoir was even lower at 0·4–0·5 during June and July of 2006 and 2007 (calculated from Heilweil *et al.*, 2009a, Table II). The use of trench infiltration techniques for managed aquifer recharge in warm arid climates, therefore, would greatly reduce evaporative losses and improve water-use efficiency. Also, with an excavation cost of $20 per linear meter plus trench materials and water-supply plumbing, the total construction cost of the trench was about $5000 USD, or about $150 per m^3/day of infiltration. This compares favorably with the use of injection wells for ASR, which deliver water at an average cost of about $300 per m^3/day (RD Pyne, written commun., 2009).

CONCLUSIONS

The use of trench infiltration has been shown to cost-effectively deliver recharge to an outcropping sandstone aquifer in southwestern Utah. Artificial recharge rates using this method were much higher than applying recharge to the same aquifer using surface-spreading techniques. In addition, trench infiltration greatly reduced evaporative losses and improved water-use efficiency in this warm climate. There are many other potential sites for this type of managed aquifer recharge to the Navajo Sandstone throughout the Colorado Plateau of the western United States. In addition, there are several other large eolian sandstone formations that could potentially be targeted for trench infiltration, such as the Mercosul aquifer system of South America (areal extent of 1 200 000 km^2; Araujo *et al.*, 1999) and the Nubian Sandstone of northeast Africa (areal extent of 2 200 000 km^2; Bakhbakhi, 2006). Considerations for applying this trench infiltration method to other sandstone aquifers include primary and fracture permeability, seasonal variation in air temperature, degree of secondary caliche deposition, suspended-sediment load of source water, water quality differences

between recharge and native groundwater, and depth to the underlying regional water table.

ACKNOWLEDGEMENTS

This study was funded by the Washington County Water Conservancy District in cooperation with the U.S. Geological Survey. Publication is authorized by the Director of the U.S. Geological Survey. The authors thank Joel Hubbell and Buck Sisson, Idaho National Laboratory, for their technical assistance with installing the advanced tensiometers; and Kevin Ellett, U.S. Geological Survey, for his technical assistance calibrating and installing the heat dissipation probes.

REFERENCES

Araújo LM, Franca AB, Potter PE. 1999. Hydrogeology of the Mercosul aquifer system in the Paraná and Chaco-Paraná Basins, South America, and comparison with the Navajo-Nugget aquifer system, USA. *Hydrogeology Journal* **7**: 317–336.

Bakhbakhi M. 2006. Nubian Sandstone Aquifer System. In *Non-renewable groundwater resources: a guidebook on socially sustainable management for water-policy makers*, vol. 10, Foster S, Loucks DP (eds). United Nations Educational: *Scientific, and Cultural Organization IHP-VI series on Groundwater* 10, Paris; 75–81.

Barnett TP, Pierce DW. 2008. When will Lake Mead go dry? *Water Resources Research.* DOI: 10.1029/2007WR006704.

Baveye P, Vandevivere P, Hoyle BL, DeLeo PC, Lozada DS. 1998. Environmental impact and mechanisms of the biological clogging of saturated soils and aquifer materials. *Critical Reviews in Environmental Science and Technology* **28**(2): 123–191.

Beckwith CW, Baird AJ. 2001. Effect of biogenic gas bubbles on water flow through poorly decomposed blanket peat. *Water Resources Research* **37**(3): 551–558.

Bouwer H. 1996. Issues in artificial recharge. *Water Science and Technology* **33**(10, 11): 381–390.

Bouwer H, Rice RC. 1984. Renovation of wastewater at the 23rd Avenue rapid-infiltration project, Phoenix, AZ. *Journal of the Water Pollution Control Federation* **56**(1): 76–83.

Bouwer H, Rice RC. 1989. Effect of water depth in groundwater recharge basins on infiltration. *Journal of Irrigation and Drainage Engineering* **115**(4): 556–567.

Brand CC. 2008. An ASR primer. *Southwest Hydrology* **7**(3): 16–17.

Bristow K, Campbell L, Gaylon S, Calissendorff K. 1993. Test of a heat-pulse probe for measuring changes in soil water content. *Soil Science Society of America Journal* **57**(4): 930.

Chadha DK. 2000. *Rain Water Harvesting and Artificial Recharge to Ground Water—A Guide to Follow*. UNESCO International Hydrology Programme Non Serial Publications in Hydrology: New Delhi, India; 22.

Cho WJ, Lee JO, Chun KS. 1999. The temperature effects on hydraulic conductivity of compacted bentonite. *Applied Clay Science* **14**: 47–58.

Christiansen JE. 1944. Effect of entrapped air upon the permeability of soils. *Soil Science* **58**(5): 355–365.

Constantz J, Herkelrath WN, Murphy F. 1988. Air encapsulation during infiltration. *Soil Science Society of America Journal* **52**: 10–16.

Cordova RM. 1978. Ground-water conditions in the Navajo Sandstone in the central Virgin River basin, Utah. *State of Utah Department of Natural Resources Technical Publication* **61**: 66.

Dagès C, Voltz M, Lacas JG, Huttel O, Negro S, Louchart X. 2008. An experimental study of water table recharge by seepage losses from a ditch with intermittent flow. *Hydrological Processes* **22**: 3555–3563.

Dillon P. 2005. Future management of aquifer recharge. *Hydrogeology Journal* **13**: 313–316.

Dillon P. 2009. Water recycling via managed aquifer recharge in Australia. *Boletín Geolígico y Minero* **120**(2): 215–234.

Dilyunas IP. 1976. Experience in artificial groundwater recharge for water supply in Lithuania. *Soviet Hydrology, Selected Papers* **15**: 340–343.

Escalante EF, Garcia JM, Minaya MJ. 2009. Proposal for the detection and correction of impacts produced by clogging processes in the Cubeta de Santiuste artificial recharge facilities (Segovia, Spain). *Boletín Geolígico y Minero* **120**(2): 215–234.

Faybishenko BA. 1995. Hydraulic behavior of quasi-saturated soils in the presence of entrapped air: Laboratory experiments. *Water Resources Research* **31**(10): 2421–2435.

Freethey GW. 1988. *Geohydrology of the Navajo Sandstone in western Kane, southwestern Garfield, and southeastern Iron Counties, Utah*. Report **88-4040**. U.S. Geological Survey Water-Resources Investigations; 43.

Gale I, Dillon P. 2005. Strategies for managed aquifer recharge (MAR) in semi-arid areas. *UNESCO International Hydrological Programme* 30.

Hantke HH, Schlegel W. 1995. The use of seepage trenches for artificial groundwater recharge. *In Artificial Recharge of Ground Water II*, *Proceedings of the 2nd International Symposium on Artificial Recharge of Ground Water*, Johnson AI, Pyne RD (eds).Walt Disney World: Florida, July 17–22, 1994, 177–187.

Heilweil VM, Freethey GW. 1992. *Simulation of ground-water flow and water-level declines that could be caused by proposed withdrawals, Navajo Sandstone, southwestern Utah and northwestern Arizona*. Report **90-4105**. U.S. Geological Survey Scientific Investigations; 51.

Heilweil VM, Freethey GW, Stolp BJ, Wilkowske CD, and Wilberg DE. 2000. *Geohydrology and numerical simulation of ground-water flow in the central Virgin River basin of Iron and Washington Counties, Utah*. Utah Department of Natural Resources Technical Publication **116**: 182.

Heilweil VM, Hsieh PA. 2006. Determining anisotropic transmissivity using a simplified Papodopulos method. *Ground Water* **44**(5): 749–753.

Heilweil VM, McKinney TS, Zhdanov MS, Watt DE. 2007. Controls on the variability of net infiltration to desert sandstone. *Water Resources Research* **43**: W07431. DOI:10.1029/2006WR005113.

Heilweil VM, Ortiz G, Susong DD. 2009a. *Assessment of managed aquifer recharge at Sand Hollow Reservoir, Washington County, Utah, updated to conditions through 2007*. U.S. Geological Survey Scientific Investigations Report **2009-5050**: 20.

Heilweil VM, Solomon DK. 2004. Millimeter- to kilometer-scale variations in vadose-zone bedrock solutes: Implications for estimating recharge in arid settings. In *Ground-water Recharge in a Desert Environment: The Southwestern United States*, Water Science and Application 9, Phillips F, Scanlon B, and Hogan J (eds). American Geophysical Union: Washington, DC; 49–67.

Heilweil VM, Solomon DK, Ortiz G. 2009b. Silt and gas accumulation beneath an artificial recharge spreading basin, southwestern Utah, USA. *Boletín Geolígico y Minero* **120**(2): 7–16.

Heilweil VM, Solomon DK, Perkins KS, Ellett KM. 2004. Gas-partitioning tracer test to quantify trapped gas during recharge. *Groundwater* **42**(4): 589–600.

Heilweil VM, Susong DD, Gardner PM, Watt DE. 2005. *Pre- and post-reservoir ground-water conditions and assessment of artificial recharge at Sand Hollow, Washington County, Utah, 1995–2005*. U.S. Geological Survey Scientific Investigations Report ***2005-5185***; 74.

Hiscock KM, Grischek T. 2002. Attenuation of groundwater pollution by bank filtration. *Journal of Hydrology* **266**: 139–144.

Hubbell JM, Sisson JB. 1998. Advanced tensiometer for shallow or deep soil water potential measurements. *Soil Science* **163**(4): 271–277.

Hurlow HA. 1998. *The geology of the central Virgin River basin, southwestern Utah, and its relation to ground-water conditions*. Utah Geological Survey Water Resources Bulletin, **26**, Utah Department of Natural Resources: Salt Lake City, Utah.

Katznelson R. 1989. Clogging of groundwater recharge basins by cyanobacterial mats. *FEMS Microbiology Ecology* **62**: 231–242.

Massmann G, Sültenfuß J. 2008. Identification of processes affecting excess air formation during natural bank filtration and managed aquifer recharge. *Journal of Hydrology* **359**: 235–246.

Mhamdi R, Heilweil VM. 2007. A quantitative evaluation of the impacts of artificial recharge to the Mornag aquifer system of northern Tunisia. In *Management of Aquifer Recharge for Sustainability*, Fox P (ed). Acacia Publications: Phoenix, Arizona; 484–493.

Morton FI. 1983. Operational estimates of lake evaporation. *Journal of Hydrology* **66**: 77–100.

National Research Council. 2008. *Prospects for managed underground storage of recoverable water*, ISBN-10: 0-309-11438-1. National Academy Press: 350.

Oberdorfer JA, Peterson FL. 1985. Waste-water injection: geochemical and biogeochemical clogging processes. *Ground Water* **23**: 753–761.

Paulson LJ. 1983. Use of hydroelectric dams to control evaporation and salinity in the Colorado River System. In *Proceedings of the 1981 Symposium on the Aquatic Resources Management of the Colorado River Ecosystem*, November 16–18, 1981, Las Vegas, NV. Ann Arbor Science, Ann Arbor, MI: 439–456.

Pyne RDG. 2005. *Aquifer Storage and Recovery: A Guide to Groundwater Recharge Through Wells*, 2nd ed. ASR Press: 620.

Reese RS. 2001. *Inventory and review of aquifer storage and recovery in southern Florida*. U.S. Geological Survey Water-Resources Investigations Report ***02-4036***; 56.

Rice RC. 1974. Soil clogging during infiltration of secondary effluent. *Journal of the Water Pollution Control Federation* **46**(4): 708–716.

Rinck-Pfeiffer S, Raqusa S, Sztainbok P, Vandevelde T. 2000. Interrelationships between biological, chemical, and physical processes as an analog to clogging in aquifer storage and recovery. *Water Resources Research* **34**(1): 2110–2118.

Robson SG, Banta ER. 1995. *Ground water atlas of the United States: Arizona, Colorado, New Mexico, and Utah*. U.S. Geological Survey Hydrologic Atlas **730-C**.

Schuh WM. 1988. In-situ method for monitoring layered hydraulic impedance development during artificial recharge with turbid water. *Journal of Hydrology* **101**: 173–189.

Schuh WM. 1990. Seasonal variation of clogging of an artificial recharge basin in a northern climate. *Journal of Hydrology* **121**: 193–215.

Smith HP. 1967. Artificial recharge and its potential in Illinois. *I.A.S.H. Symposium of Haifa*; 13b-m.

Uygur K. 1980. *Hydraulic and petrographic characteristics of the Navajo Sandstone in southern Utah: Salt Lake City*. University of Utah Department of Geology and Geophysics Master's Thesis; 134.

Waddington JM, Ketcheson SJ, Kellner E, Strack M, Baird AJ. 2009. Evidence that piezometers vent gas from peat soils and implications for pore-water pressure and hydraulic conductivity measurements. *Hydrological Processes* **23**: 1249–1254.

Weiss RF. 1970. The solubility of nitrogen, oxygen and argon in water and seawater. *Deep Sea Research and Oceanographic Abstracts* **17**(4): 721–735.